

A Study of Trajectory Simulation of Master Arm

Jin-Soo Moon*

Abstract

In industrial fields, human works are being replaced by robots. However, as the use of robots is limited in the process industry where they are operated fixedly, humanoid robots with wide applications need to be developed. Currently a great deal of research is being conducted on humanoid robots with the object of replacing humans in the workplace. However, because of the lack of relevant hardware and difficulty in mechanical parts, only very simple and limited progress is being made. In an effort to overcome these limitations, the purpose of the present study is to develop a kinematical mechanism and a controller. To this end, master arms with 3 degrees-of-freedom for the shoulders and the arms were composed which were able to reproduce human-like motions by simulating the characteristics of joint variables and the trajectory of the end-effector.

Key Words : Master arm, Denavit-Hartenberg, Trajectory, End-effector

1. Introduction

The demand for robots has gradually increased in order to eliminate the notorious three Ds (Difficult, Dangerous and Dirty) in the industries and improve productivity. The use of robots was previously limited to the process industry. However, moving robots have recently been preferred due to their multiple uses. Even if most robots use wheels or endless trajectory to keep their balance, they are very restricted by obstacles and topography. Therefore, many studies have

been conducted on humanoid robots in terms of kinematics and kinetics [1-5].

The shape of the human body is closely related to the bones that are connected to each other at joints. Therefore, body motion is decided by the change in direction and position of bones around each joint.

In the human body model, the tract can be generated by designating the shape of bones and changing joint attributes. In fact, human bones and joints have complicated structures with a high degree of freedom. In robot modeling, on the contrary, the degree of freedom cannot be entirely expressed. Therefore, a simple model is used to get the minimum degree of freedom. Even though more specific and more detailed motions can be made as more joints are used, the calculations become more complicated accordingly [6].

* Main author : Department of Robot Engineering,
Busan Human Resources
Development Institute

Tel : +82-51-610-3170, Fax : +82-51-626-4293

E-mail : jsm@korcham.net

Date of submit : 2007. 7. 9

First assessment : 2007. 7. 16, Second : 2007. 8. 28

Completion of assessment : 2007. 10. 12

This paper uses a three degrees of freedom mechanism for the master arm and aims to simulate the characteristics of joint variables and the trajectory of the end-effector (the end point of the robot in which operation can be performed with tools) [7-8].

2. Kinematic Analysis

In general, a master arm robot consists of a head, body and arms. Here, arm motion can be divided into a 3-degrees-of-freedom shoulder, 1 degree of freedom elbow and 3 degrees of freedom wrist. Therefore, it's desirable to design 7 axes for one arm. Since the rotary joint in the shoulder and wrist can not be attached to the central axis of the shoulder and wrist and the wrist rotates around the same position, kinematic interference occurs [9].

To eliminate this kind of interference and simulate human movement, the structure of the 3-degrees-of-freedom master arm consists of two axes for the shoulder and 1 axis for the elbow as shown in Fig. 1 below and sets the coordinates as follows: master arm connecting rotational axis: θ_1 , shoulder rotational axis: θ_2 , and elbow rotational axis: θ_3 . If Denavit-Hartenberg (D-H) parameters are used for kinematic analysis of the master arm robot, the coordinate transformation equation of joints shall be stated as follows:

$${}^nT_{n+1} = A_{n+1} = \begin{matrix} Rot(z, \theta_{n+1}) \\ \times Trans(0, 0, d_{n+1}) \\ \times Trans(a_{n+1}, 0, 0) \\ \times Rot(x, \alpha_{n+1}) \end{matrix} \quad (1)$$

In D-H representation, all joints can be expressed around a Z axis. Then, the Z axis becomes the rotational joint. The linear moving direction of the translational joint becomes Z axis, X · Y axes are determined depending on Euler's coordinate. Therefore, the D-H parameter for the

analysis of robotic kinematics shall be stated as shown in Table 1 below: [9, 10].

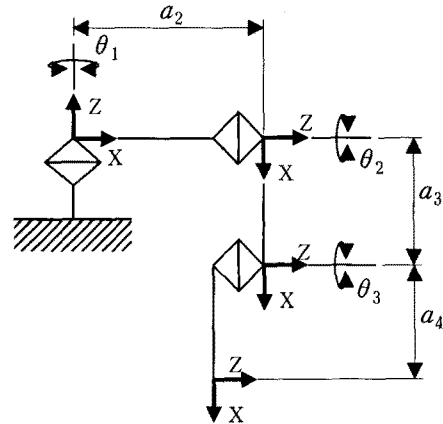


Fig. 1. Kinematic Structure of Master Arm

In Table 1, parameter θ refers to the rotational angle of each axis and d represents axial travel while a refers to a length of link and α represents the torsion angle of the Z axis.

Table 1. D-H Parameter of Master Arm

	θ	d	a	α
Joint1	θ_1	0	0	0
Joint2	θ_2	0	a_2	-90
Joint3	θ_3	0	a_3	0
Joint4	0	0	a_4	0

Here, to simplify sin and cos, $\sin \theta_n$ and $\cos \theta_n$ were stated as S_n and C_n respectively. Then, the conversion transformation of each joint on coordinate transformation shall be stated as follows:

$$A_1 = Rot(z, \theta_1) \quad (2)$$

$$A_2 = \begin{matrix} Rot(z, \theta_2) \\ \times Trans(a_2, 0, 0) \times Rot(x, -90) \end{matrix} \quad (3)$$

$$A_3 = Rot(z, \theta_3) \times Trans(a_3, 0, 0) \quad (4)$$

$$A_4 = Trans(a_4, 0, 0) \tag{5}$$

In terms of forward kinematics, the multiplication of the entire matrix can be stated as follows:

$$\begin{aligned} {}^0T_4 &= A_1 A_2 A_3 A_4 \\ &= \begin{bmatrix} C_1 & -S_1 & 0 & 0 \\ S_1 & C_1 & 0 & 0 \\ 0 & 0 & 1 & 0 \\ 0 & 0 & 0 & 1 \end{bmatrix} \times \begin{bmatrix} C_2 & 0 & -S_2 & C_2 a_2 \\ S_2 & 0 & C_2 & S_2 a_2 \\ 0 & -1 & 0 & 0 \\ 0 & 0 & 0 & 1 \end{bmatrix} \\ &\quad \times \begin{bmatrix} C_3 & -S_3 & 0 & C_3 a_3 \\ S_3 & C_3 & 0 & S_3 a_3 \\ 0 & 0 & 1 & 0 \\ 0 & 0 & 0 & 1 \end{bmatrix} \times \begin{bmatrix} 1 & 0 & 0 & a_4 \\ 0 & 1 & 0 & 0 \\ 0 & 0 & 1 & 0 \\ 0 & 0 & 0 & 1 \end{bmatrix} \\ &= \begin{bmatrix} C_{123} & -C_{12}S_3 & -S_{12} & C_{12}(C_3a_4 + C_3a_3 + a_2) \\ S_{12}C_3 & -S_{12}S_3 & C_{12} & S_{12}(C_3a_4 + C_3a_3 + a_2) \\ -S_3 & -C_3 & 0 & -S_3a_4 - S_3a_3 \\ 0 & 0 & 0 & 1 \end{bmatrix} \end{aligned} \tag{6}$$

The criterion coordinate of the robot can be defined as follows:

$${}^0T_4 = \begin{bmatrix} n_x & o_x & a_x & P_x \\ n_y & o_y & a_y & P_y \\ n_z & o_z & a_z & P_z \\ 0 & 0 & 0 & 1 \end{bmatrix} \tag{7}$$

Here, each variable can be stated as the following equations:

$$P_x = C_{12}(C_3a_4 + C_3a_3 + a_2) \tag{8}$$

$$P_y = S_{12}(C_3a_4 + C_3a_3 + a_2) \tag{9}$$

$$P_z = -S_3a_4 - S_3a_3 \tag{10}$$

To find out the coordinate x, y, z of the end-effector, the end-effector trajectory at the angle of each joint (θ) is set to P_x, P_y and P_z [10].

3. Configuration of Experimental Device

A humanoid robot is designed to be mid-sized: 85[cm] in height, 30[cm] of arm's length, 20[kg] in

weight. Having legs with 5 degrees of freedom, walking forward and backward is possible. By designing it with a camera on the head, it is equipped with an image recognition function as well.

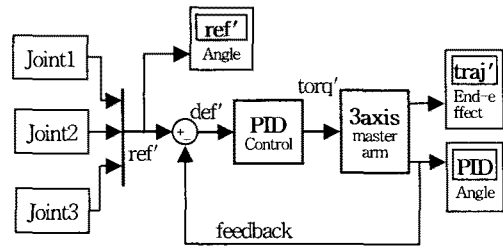


Fig. 2. Block Diagram of Simulation

Two ultrasonic sensors are equipped to detect forward obstacles, and 1 degree of freedom was used for free neck joint movement. With a 2-degrees-of-freedom pitch-roll shoulder and a 1 degree of freedom pitch arm, furthermore, the arm is designed to simulate human motion.

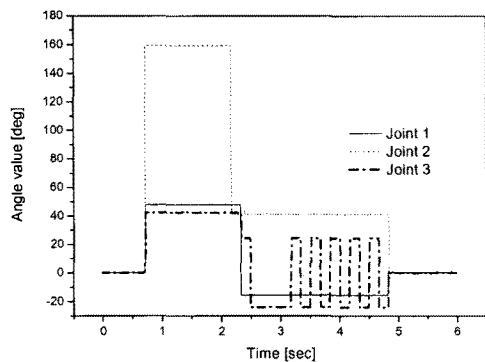


Fig. 3. Parameters of Reference Angle

Fig. 2 shows a block diagram for simulation of end-effect trajectory. The reference angle in each joint has adopted PICO ADC-200 Model of Virtual Instrument and sampling data have been acquired at every 5ms.

The acquired data are demonstrated on the time

A Study of Trajectory Simulation of Master Arm

axes (the angles of connecting rotational axis θ_1 , shoulder rotational axis θ_2 and elbow rotational axis θ_3 to angle values of Joint 1 through Joint 3) as shown in Fig. 3.

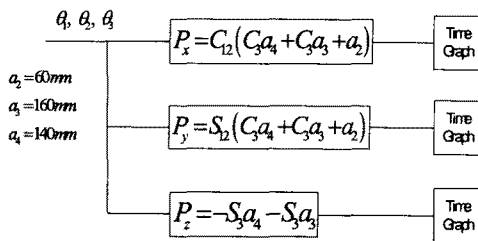


Fig. 4. Block Diagram of Kinematics

Fig. 4 shows the block diagrams of Equation (8)~ Equation (10) to create the trajectory of a robot arm end-effector. For input data, $a_2=60$ [mm], $a_3=160$ [mm] and $a_4=140$ [mm] that are applied to the design of the master arm are entered and the angle trajectory of each joint in θ_1 , θ_2 and θ_3 .

4. Simulation

Fig. 5 through Fig. 9 show the trajectory simulation of the master arm end-effector. The reference angles of Joint 1 through Joint 3 in Fig. 3 were estimated using PID simulation.

Table 2. Parameters of DC motor

Sign	Description	Value	Unit
R_m	Armature Resistance	8.57	Ω
L_m	Armature Inductance	0.16	mH
J_m	Armature Rotation Inertia	2.84×10^{-7}	$kg \cdot m^2$
K_m	Counter Electromotive Force	0.0061	$V/rad/sec$
K_t	Torque Constant	0.0061	$N \cdot m/A$

Table 2 shows parameters of DC motor while Table 3 represents parameters of PID characteristics. For simulation, the response characteristics on each displacement have been estimated against the master arms ($\theta_1 \sim \theta_3$) in Fig. 1. Based on the reference angle in Fig. 3, the parameters of PID characteristics in Table 2 have been applied. The followings results (Fig. 5 through Fig. 7) have been acquired.

Table 3. Parameters of PID characteristics

	P	I	D
Joint1	300	40	8
Joint2	61	24	2
Joint3	43	11	2

In Fig. 5, the reference angle from joint variable in Joint 1 is parameters from MPU while the simulation value (PID control angle) shows the test result of PID parameter in Table 2.

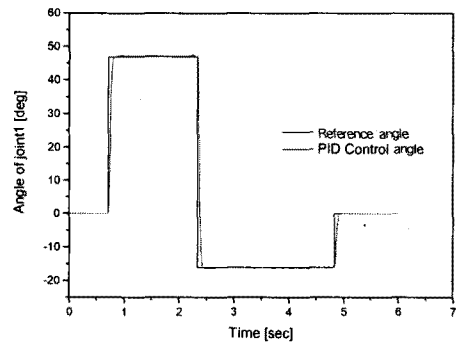


Fig. 5. Angle of No.1 Joint

In this test, the angle trajectory in Joint 1 had the same results as the reference angle. In Joint 1, the rotational axis connected to the robot arm, and relatively stable characteristics were confirmed due to low load and simple motions.

In Joint 2 angle trajectory in Fig. 6, the load is directly applied to the arm axis. Therefore, the

response time to reach the target value was late and unstable motions were observed. In addition, error span was much larger than in Joint 1.

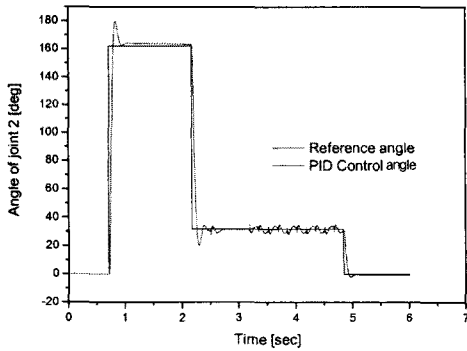


Fig. 6. Angle of No.2 Joint

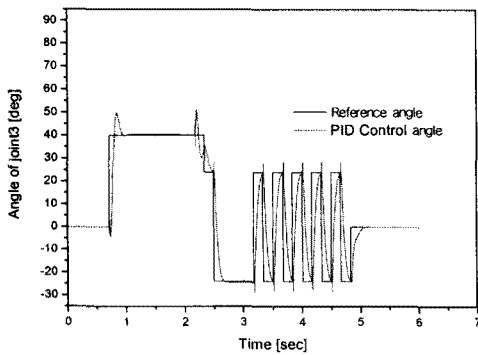


Fig. 7. Angle of No.3 joint

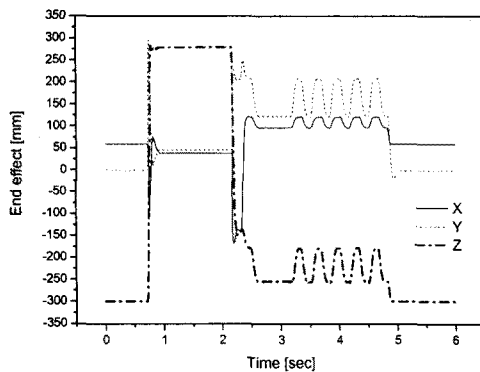


Fig. 8. Simulation Trajectory of End-effector

Even though the angle trajectory of Joint 3 in Fig. 7 has the same arm as Joint 2, the wrist is included. Therefore, the target value has been safely reached. However, the next motion was made before target value was reached in intermittent motion. For this reason, the response was late and the error span was wide.

Fig. 8 shows 3D trajectory characteristics by applying PID control angles from Fig. 5 through Fig. 7 to the block diagram of kinematics in Fig. 4. Because of end-effector trajectory traced to X, Y and Z depending on the variables of an individual angle (θ) of the kinematics of the robot, the accurate position of the coordinate can be traced. Therefore, precise and accurate position design was possible.

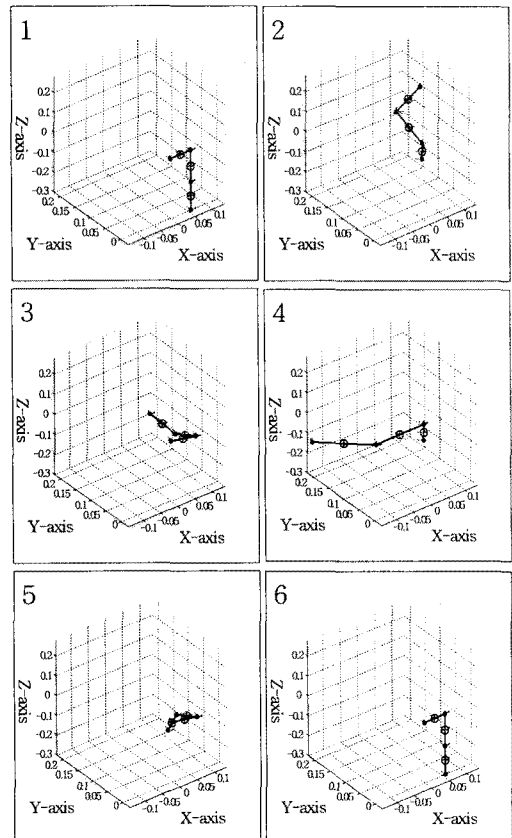


Fig. 9. Virtual Model of Simulink

Fig. 9 demonstrates the virtual motion of robot arms using the D-H parameters in Table 1. With the division of the motion of robots into 6 parts, motion patterns can be predicted.

5. Conclusion

To develop a master arm for a humanoid robot, master arm with a 3-degrees-of-freedom has been designed and the characteristics of joint variables of the robot and the end-effector trajectory have been simulated.

In this test, the motion could be predicted only with parameters. They were useful in the production of industrial robot routes. As discovered in the test of the characteristics of joint variables, however, trajectory torsion has been observed at acceleration and the response characteristics and iterative precision were insufficient.

Therefore, a humanoid robot will be developed by complementing the weaknesses discovered in this paper and making use of the characteristics of the already developed trajectory.

References

[1] Y. W. Sung and S. Y. Yi, "The Development of a Miniature Humanoid Robot System", *Journal of Control, Automation and Systems Engineering*, Vol.7, No. 5, pp.420~426, 2001. 5.

[2] B. J. Oh, "A Study on a Control of 3D Animation for Adaptive Control" Ministry of Information and Communication republic of Korea, 1999.

[3] J. W. Lee, Y. S. Kim, S. Y. Lee and M. S. Kim, "Kinematic Design and Analysis of Masterarm with Distributed Controller Architecture", *Journal of Control, Automation and Systems Engineering*, Vol.7, No.6, pp.532~359, 2001. 6.

[4] J. S. Moon and C. U. Kim, "A study on Development of Actuator for Biped Walking Robot", *Journal of The Korean Institute of Illuminating and Electrical Installation Engineers* Vol. 19, No.7, pp.73~80, 2005. 11.

[5] J. S. Moon and C. U. Kim, "A Study on a Trajectory of Mast Arm End-Effector", *Journal of The Korean Institute of Illuminating and Electrical Installation Engineers* Vol. 20, No.10, pp.151~157, December 2006.

[6] T. B. Sheridan, *Telerobotics, Automation, and Human Supervisory Control*, The MIT Press, Cambridge, MA, 1992.

[7] J. G. Jin, J. Sakong, J. Y. Choi, "Learning and Generation of Motion Trajectory in a Humanoid Robot", *Proceeding of KFS2001 Spring Conference*, 2001. 5.

[8] S. H. Yi, S. H. Yang, Y. K. Park, "Generation of Constant Orientation in Industrial Robots", *Transaction of the Korean Society of Machine Tool Engineers*. Vol. 10 No. 2, 2001. 4.

[9] Y. S. Kim, J. W. Lee, S. Y. Lee, M. S. Kim, J. W. Lee, "Masterarm Development for Teleoperation of a Humanoid Robot", *The Korean Institute of Electrical Engineers*. Vol. 50D No. 6, 2001. 6.

[10] Mark W. Spong, M. Vidyasagar, "Robot Dynamics and Control", John wily & sons, Inc. 1989.

Biography

Jin-Soo Moon

Received the M.S. degree in electrical engineering in 2003 and the Ph.D. degree in 2008 from Pusan National University, Busan, Korea. He has been a Professor at Busan Human Resources Development Institute run by The Korea Chamber of Commerce & Industry.